Research note

Evolution of the ring current energy during May 2–4, 1998 magnetic storm

Natalia Yu. Ganushkina[1], Jussi Korhonen[2], Tuija I. Pulkkinen[1], Yusuke Ebihara[3], Masaki Ejiri[3] and Ted Fritz[4]

[1] *Finnish Meteorological Institute, Geophysical Research Division,*
P.O. Box 503, FIN-00101 Helsinki, Finland
[2] *University of Helsinki, Helsinki, Finland*
[3] *National Institute of Polar Research, Kaga 1-chome, Itabashi-ku, Tokyo 173-8515*
[4] *Boston University, Department of Astronomy, Boston, MA, U.S.A.*

Abstract: We study the evolution of the ring current energy density during May 2–4, 1998 storm event as measured by Polar CAMMICE/MICS instrument and modelled by proton tracing in the guiding center approximation. Particle data from Polar shows that during the storm main phase protons with medium energies (20–80 keV) contribute more to the total ring current energy than the high energy protons (80–200 keV) whereas during the recovery phase high energies dominate. We trace protons with arbitrary pitch angles numerically in the guiding center approximation taking into account charge-exchange losses. Tracing is performed in the large-scale and smaller-scale time-dependent magnetic and electric field models. We model the substorm activity by several electric field pulses at times of the substorm onsets. It is shown that impulsive electric fields associated with substorms are effective in the proton transport and energization to higher energies more than 100 keV in the storm time ring current.

1. Introduction

A signature of a magnetic storm is a depression in the *Dst* index caused by the enhancement of the ring current, which corresponds to a factor of ten increase in the energy content of the trapped particle population lasting over ten hours. The main contribution to *Dst* comes from particles in the 10–200 keV energy range, these contribute majority of the energy content in the geomagnetically trapped particles.

The basic transport and acceleration process for ions moving from the magnetotail and the plasma sheet to the inner magnetosphere is the $\mathbf{E} \times \mathbf{B}$ drift imposed by the large-scale electric field in the nightside magnetosphere. In the magnetotail the particles gain energy while they move from regions of weaker to stronger magnetic field, conserving their first adiabatic invariant. While approaching the inner magnetosphere, the particles are transported across magnetic field lines primarily by gradient and curvature drift, as well as by $\mathbf{E} \times \mathbf{B}$

drift in a complicated combination of potential and induction electric fields.

The question of the relative importance of the large-scale convection electric field and the substorm-associated impulsive electric fields in the energization and transport of ions into the ring current is still open. This is closely related to the storm-substorm relationship issue. Earlier studies (Chapman, 1962; Akasofu, 1968) considered storms as the result of a superposition of successive substorms. Recently, several studies have opposed this view concluding that substorm occurrence is incidental to the main phase of storms, and that ion transport into the ring current is accomplished solely by enhanced large-scale convection electric fields (see, for example, the studies by Kamide *et al*., 1998; Daglis *et al*., 2003).

Substorm-associated electric field usually displays a very complicated behaviour with a strong pulsed component (Maynard *et al*., 1996). Large transient electric fields exist in the plasma sheet during the substorm expansion phase (Aggson *et al*., 1983; Tu *et al*., 2000; Rowland and Wygant, 1998). Rather intense (a few mV/m) electric fields have been detected very deep in the inner magnetosphere, inside the plasmasphere. The origin of strong transient electric fields at substorm onset and their relationship to the magnetic field dipolarization is still an open question.

Model of an earthward propagating electromagnetic field pulse (Li *et al*., 1998; Zaharia *et al*., 2000; Sarris *et al*., 2002) has been proposed to explain the particle injections during substorms: particles are energized by betatron mechanism (magnetic moment is conserved) as they are shifted by the pulse to regions with higher magnetic field closer to the Earth. Analysis of single-particle dynamics in simulations of magnetospheric field reconfigurations has revealed prominent acceleration of plasma sheet ions during the expansion phase of substorms (Delcourt, 2002). The high energies reached by ring current ions can be accounted for by the action of substorm-associated impulsive electric fields (Ganushkina *et al*., 2001). These accelerated ions provide a significant part of the ring current. Although there are many models of the ring current development (for example, Ebihara and Ejiri, 2000; Fok *et al*., 1999; Chen *et al*., 1994; Jordanova *et al*., 1994), and initial efforts of incorporating of impulsive electromagnetic fields into the ring current modelling have been done (Ganushkina and Pulkkinen, 2002) the detailed relation and possible combined action of convection and induction electric fields has still to be explored.

In the present paper we study the evolution of the ring current energy during May 2–4, 1998 storm event as measured by Polar CAMMICE/MICS instrument and modelled by proton tracing in the guiding center approximation. Evolution of contributions from protons with different energy ranges such as total (1–200 keV), low (1–20 keV), medium (20–80 keV) and high (80–200 keV) energies to the total energy of the ring current during different storm phases is followed. We trace protons with arbitrary pitch angles numerically in the large-scale and smaller scale time-dependent magnetic and electric field models in the guiding center approximation taking into account charge-exchange losses. We model the substorm activity by several electric field pulses at times of the substorm onsets. We address the question about the effectiveness of impulsive electric fields associated with substorms in the proton transport and energization to higher energies ($>$80 keV) in the storm time ring current. The formation of the ring current as a combination of large-scale convection and pulsed inward shift and consequent energization of the ring current particles is discussed.

2. Description of May 2–4, 1998 storm event

The storm in early May 1998, was initiated from an extended period of solar activity which started on April 29, 1998. There were several coronal mass ejections during the period: on April 29 (1700 UT), May 1 (2340 UT), May 2 (0530 UT) and May 4 (0200 UT). Here we concentrate on the period from May 2 to May 4, 1998. Figure 1 shows (panels from top to bottom) the interplanetary magnetic field (IMF) B_z component, the solar wind dynamic pressure P_{sw} as obtained from WIND measurements, and *AE* and *Dst* indices. The activity on May 2, 1998 was driven by a magnetic cloud, whose effects were first seen at about 0335 UT when IMF B_z turned southward. After 0335 UT, IMF B_z fluctuated close to zero until about 0800 UT, then turned southward and remained at about −10 nT until the end of May 3. The strongest period of activity occurred on May 4, when IMF B_z decreased sharply at about 0230 UT down to −30 nT, remained there for about three hours, and then increased and fluctuated around zero until the end of May 4. There were several pressure pulses, about 15 nPa during May 2, about 20 nPa in the beginning of May 3, and the highest peaks of 40 nPa around 0400 UT and 30 nPa around 0800 UT on May 4. As was shown by Russell *et al.* (2000), during the period between 0400–0800 UT the magnetopause crossed geosynchronous orbit repeatedly, getting as close as 5 R_E in the subsolar region. The magnetospheric response was seen as a strong increase in the *AE* index that reached over 2000 nT at about 1200 UT on May 2 and at about 0400 UT on May 4. There were several smaller peaks with about 1000 nT magnitude during May 2 and May 3. The *Dst* index reached −80 nT at 1500 UT on May 2 and recovered to the level of about −50 nT by the end of the day. On May 4, *Dst* dropped to −250 nT, followed by a slow recovery toward a more quiet-time state.
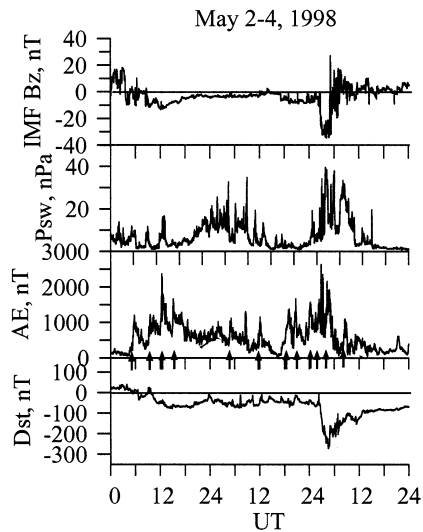
Fig. 1.   *Overview of May 2–4, 1998 storm event (panels from top to bottom): the interplanetary magnetic field (IMF) B_z component, the solar wind dynamic pressure P_{sw} as measured by WIND, and AE and Dst indices. The arrows indicate the times of substorm onsets correspondent to the action of electric field pulses.*

3. POLAR CAMMICE/MICS measurements

The Polar spacecraft was launched on an 86° inclination elliptical orbit with a 9 R_E apogee, 1.8 R_E perigee, and 18-hour orbital period. The orbit apogee was over the northern polar region. The Charge and Mass Magnetospheric Ion Composition Experiment (CAMMICE) on board Polar was designed to measure the charge and mass composition of particles within the Earth's magnetosphere over the energy range of 6 keV/Q to 60 MeV/Q (Wilken *et al*., 1992). The Magnetospheric Ion Composition Sensor (MICS) sensor identifies each ion from measurements of time of flight, energy per charge, and total energy. The counts of the major ion species are accumulated into scalers, with a full 32-channel energy spectrum in the range of 1–200 keV/Q being telemetered once every 202 s.

We used the proton energy *versus* time spectrograms from Polar CAMMICE/MICS energy range to calculate the energy density of ring current protons,

$$w\,(L) = 2\pi\sqrt{2mq} \int \sqrt{E}\,j\,(E,L)\,\mathrm{d}E,$$

where m is the proton mass, q is the proton charge state, E is the energy and j is the measured proton differential flux, and total proton ring current energy,

$$W_{RC} = \int_V w\,(L)\,\mathrm{d}V,\ \ \mathrm{d}V = 2R_E^3 L^2\sqrt{1 - \frac{1}{L}}\left(\frac{1}{7L^3} + \frac{6}{35L^2} + \frac{8}{35L} + \frac{16}{35}\right)\mathrm{d}L\mathrm{d}\phi,$$

where ϕ is the local time, dipole magnetic field was used. Figure 2 shows the calculated contributions to the total proton ring current energy (1–200 keV, circles, all panels) from
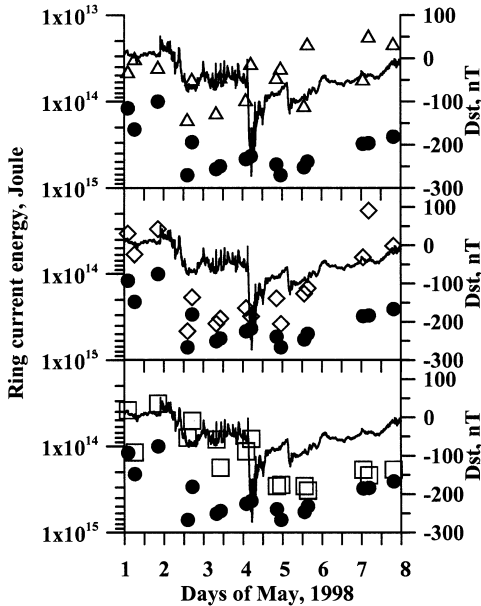

Fig. 2.   *Calculated contributions to the total proton ring current energy (1–200 keV, black circles, all panels) from low (1–20 keV, open triangles, top panel), medium (20–80 keV, open diamonds, middle panel) and high (80–200 keV, open rectangles, bottom panel) energy protons together with the measured Dst index (all panels) during the period of May 1–7, 1998.*

low (1–20 keV, open triangles, top panel), medium (20–80 keV, open diamonds, middle panel) and high (80–200 keV, open rectangles, bottom panel) energy protons together with the measured *Dst* index (all panels) during the period of May 1–7, 1998. As can be noted, the medium energy protons are the main contributors to the total ring current energy during the main phase of the storm maximum on May 4. During the recovery phase the high energy protons play a dominant role. A significant difference can be seen between measurements made at close times but in different MLT sectors which is an indicator of a large asymmetry present in the ring current (Turner *et al.*, 2001).

4. Tracing procedure description

In order to model the contributions from protons with different energies to the total ring current energy during different storm phases we traced protons with $90° \pm 60°$ pitch angles under the conservation of the 1st and 2nd invariants in different time-dependent magnetic and electric fields. As an initial distribution Maxwellian-type distribution function at $R=8$ 1900–0500 MLT. The differential flux calculations were made using Liouville's theorem. As magnetic field models the dipole and Tsyganenko T89 (Tsyganenko, 1989) models were used. As electric field models we used either *Kp*-dependent Volland-Stern convection electric field (Volland, 1973; Stern, 1975),

$$\Phi_{\text{conv}} = AR^{\gamma} \sin \phi, \ \gamma = 2, \ A = \frac{0.045}{1 - 0.159Kp + 0.0093Kp^2} \text{kV}/R_{\text{E}}^2,$$

(Maynard and Chen, 1975), where R is the radial distance, ϕ is the local time, with corotation electric field or Boyle *et al.* (1997) polar cap potential applied to Volland-Stern type convection,

$$\Phi = \left[1.1 \cdot 10^{-4} V_{\text{sw}}^2 + 11.1 B_{\text{IMF}} \sin^3 \left(\frac{\theta_{\text{IMF}}}{2} \right) \right] \frac{\sin \phi}{2} \left(\frac{R}{R_B} \right)^2, \ R_B = 10.47 R_{\text{E}},$$

where V_{sw} is the solar wind velocity, B_{IMF} is the interplanetary magnetic field intensity, θ_{IMF} is the polar angle of IMF. We introduced substorm-associated fields such as electric field pulses similar to Sarris *et al.* (2002) at substorm onsets, modeled as an electromagnetic pulse (Li *et al.*, 1998; Sarris *et al.*, 2002). Time-dependent Gaussian pulse with azimuthal electric field propagates radially inward at a decreasing velocity and decreases away from midnight. In the spherical coordinate system (r, θ, ϕ) the electric field is given by,

$$E_{\phi} = - E_0 (1 + c_1 \cos (\phi - \phi_0))^p \exp (-\xi^2),$$

where

$$\xi = \left[r - r_i + v(r)(t - t_a) \right] / d,$$

determines the location of the maximum value of the pulse, $v(r) = a + br$ is the pulse front velocity as a function of radial distance r, d is the width of the pulse, c_1 and p describe the local time dependence of the electric field amplitude, which is largest at ϕ_0,

$$t_a = (c_2 R_E / v_a)(1 - \cos(\phi - \phi_0)),$$

represents the delay of the pulse from ϕ_0 to other local times, c_2 determines the magnitude of the delay, v_a is the longitudinal propagation speed of the pulse and r_i determines the arrival time of the pulse. Following Sarris *et al*. (2002), we used $\phi_0 = 180°$, $c_1 = 1$, $c_2 = 0.5$ R_E, $a = 53.15$ km/s, $b = 0.0093$ s^{-1}, $p = 8$, $v_a = 20$ km/s, $r_i = 100$ R_E, and $d = 4 \ 10^7$ m. Time-dependent magnetic field from the pulse is calculated by Faraday's law. Loss processes such as charge-exchange with the cross sections given by Janev and Smith (1993) and the thermosphere model MSISE 90 (Hedin, 1991).

5. Modelling results

Figure 3 presents the calculated proton ring current energy in Joules (three upper panels) for four energy ranges such as the total (1–200 keV, thin solid curves), the low (1–20 keV, dash-dotted curves), the medium (20–80 keV, dotted curves) and high energies (80–200 keV, thick solid curves) and the measured *Dst* index (bottom panel) for modelled period of May 2–4, 1998. In the initial Maxwellian-type distribution the plasma sheet proton number density was $N_{ps} = 0.4$ cm^{-3} and the average temperature was 5 keV. The ring current energy curves shown in the upper panel were calculated when tracing protons in the Tsyganenko T89 magnetic field and Volland-Stern large-scale convection electric field. In this case the main contribution to the total ring current energy comes from the protons with medium energies of 20–80 keV during the whole modelled storm period. The contribution from the high energies is very small which contradicts to the observations of dominant role of the high energy protons during storm recovery phase. Next panel shows the results of the proton tracing in the Tsyganenko T89 magnetic field and the Boyle *et al*. (1997) polar cap potential applied to Volland-Stern type convection electric field. Note, that the contribution from the high energy population is rather small similar to the previous case.

To represent substorm activity during the storm on May 2–4, 1998, time varying fields associated with dipolarization in the magnetotail were incorporated, modeled as electromagnetic pulses set at substorm onset times (see Table 1). Arrows on the third panel from the top representing *AE* index in Fig. 1 mark the times when pulses occurred. Following Sarris *et al*. (2002) we set a baseline at 4 mV/m for *AE* about 1000 nT. The ratio between the electric field amplitudes is similar to the ratio between the peaks in the *AE* index during substorm onsets. The third panel from the top in Fig. 3 shows the results when proton tracing was performed in the same field models as in the previous case but with addition of electric field pulses at substorm onsets. These pulses provide the contribution from the high energy protons to be the dominant during the storm recovery phase.

6. Conclusions

We studied the evolution of contributions from protons with different energy ranges such as total (1–200 keV), low (1–20 keV), medium (20–80 keV) and high (80–200 keV) energies to the total energy of the ring current during different storm phases during May 2–4, 1998 storm event. Measurements on Polar CAMMICE/MICS instrument showed that the medium energy protons are the main contributors to the total ring current energy during
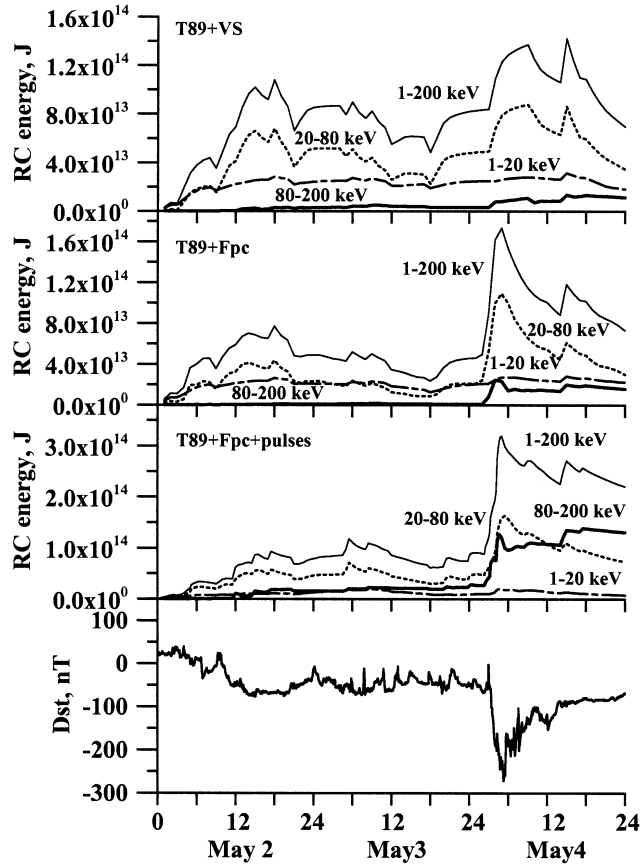
Fig. 3.   *Calculated proton ring current energy for four energy ranges such as the total (1–200 keV, thin solid curves), the low (1–20 keV, dash-dotted curves), the medium (20–80 keV, dotted curves) and high energies (80–200 keV, thick solid curves) when proton tracing was performed in different magnetic and electric field models (see the paper text) and the measured Dst index (bottom panel) for modelled period of May 2–4, 1998.*

Table 1. UTs and amplitudes of the substorm-associated electric field pulses at substorm onsets for May 2–4, 1998 storm event.

May 2, 1998		May 3, 1998		May 4, 1998	
UT	E amplitude, mV/m	UT	E amplitude, mV/m	UT	E amplitude, mV/m
0520	4	0500	3	0015	6
0910	4	1200	3	0240	6
1205	8	1800	4	0325	8
1600	6	2030	6	0430	7
				0900	3

the main phase of the storm maximum on May 4. During the recovery phase the high energy protons play a dominant role.

To model this evolution we traced protons with arbitrary pitch angles numerically in the drift approximation. Tracing was performed in the large-scale (Tsyganenko T89 magnetic and large-scale convection electric fields) and smaller-scale time-dependent magnetic and electric field models. The results of tracing protons in the Tsyganenko T89 magnetic field and large-scale convection electric fields exhibited the main contribution to the total ring current energy coming from the protons with medium energies of 20–80 keV during the whole modelled storm period. The contribution from the high energies was very small which contradicted to the observations of dominant role of the high energy protons during storm recovery phase. Time-dependent electric field was given by Gaussian electric field pulse with azimuthal field component propagating inward at a decreasing velocity. We modeled particle inward motion and energization by a series of electric field pulses representing substorm activations during storm events. It was demonstrated that such fluctuating fields can effectively energize the plasma sheet protons to the energies more than 80 keV and transport them inward to closed drift shells providing the dominant contribution to the total ring current energy during the storm recovery phase. This can mean that the formation of the ring current is a combination of large-scale convection and pulsed inward shift and consequent energization of the ring current particles.

Acknowledgments

References

Aggson, T.L., Heppner, J. and Maynard, N. (1983): Observations of large magnetospheric electric fields during the onset phase of a substorm. J. Geophys. Res., **88**, 3981–3990.

Akasofu, S.-I. (1968): Polar and Magnetospheric Substorms. Dordrecht, D. Reidel, 280 p.

Boyle, C.B., Reiff, P.H. and Hairston, M.R. (1997): Empirical polar cap potentials. J. Geophys. Res., **102**, 111–125.

Chapman, S. (1962): Earth storms: Retrospect and prospect. J. Phys. Soc. Jpn., **17**, 6–16.

Chen, M.W., Lyons, L.R. and Schultz, M. (1994): Simulation of phase space distributions of storm time proton ring current. J. Geophys. Res., **99**, 5745–5759.

Daglis, I.A., Kozyra, J.U. and Kamide, Y. (2003): Intense space storms: Critical issues and open disputes. J. Geophys. Res., **108**, 1208, doi:10.1029/2002JA009722.

Delcourt, D.C. (2002): Particle acceleration by inductive electric fields in the inner magnetosphere. J. Atmos. Sol.-Terr. Phys., **64**, 551–559.

Ebihara, Y. and Ejiri, M. (2000): Simulation study on fundamental properties of the storm-time ring current. J. Geophys. Res., **105**, 15843–15860.

Fok, M.-C., Moore, T.E. and Delcourt, D.C. (1999): Modeling of inner plasma sheet and ring current during substorms'. J. Geophys. Res., **104**, 14557–14569.

Ganushkina, N.Yu. and Pulkkinen, T.I. (2002): Particle tracing in the Earth's magnetosphere and the ring current

formation during storm times. Adv. Space Res., **30**, 1817–1820.

Ganushkina, N.Yu., Pulkkinen, T.I., Bashkirov, V.F., Baker, D.N. and Li, X. (2001): Formation of intense nose structures. Geophys. Res. Lett., **28**, 491–494.

Hedin, A.E. (1991): Extension of the MSIS thermosphere model into the middle and lower atmosphere. J. Geophys. Res., **96**, 1159–1172.

Janev, R.K. and Smith, J.J. (1993): Cross sections for collision processes of hydrogen atoms with electrons, protons, and multiply-charged ions. Atomic and Plasma-Material Interaction Data for Fusion. Vol. 4. Vienna, Int. At. Energ. Agency, 78–79.

Jordanova, V.K., Kozura, J.U., Khazanov, G.V., Nagy, A.F., Rasmussen, C.E. and Fok, M.-C. (1994): A bounce-averaged kinetic model of the ring current ion population. Geophys. Res. Lett., **21**, 2785–2788.

Kamide, Y., Baumjohan, W., Daglis, I.A. *et al*. (1998): Current understanding of magnetic storms: Storm-substorm relationships. J. Geophys. Res., **103**, 17705–17728.

Li, X., Baker, D.N., Temerin, M., Reeves, G.D. and Belian, R.D. (1998): Simulation of dispersionless injections and drift echoes of energetic electrons associated with substorms. Geophys. Res. Lett., **25**, 3763–3766.

Maynard, N.C. and Chen, A.J. (1975): Isolated cold plasma regions: Observations and their relation to possible production mechanisms. J. Geophys. Res., **80**, 1009–1013.

Maynard, N.C., Burke, W.J., Basinska, E.M. *et al*. (1996): Dynamics of the inner magnetosphere near times of substorm onsets. J. Geophys. Res., **101**, 7705–7736.

Rowland, D.E. and Wygant, J.R. (1998): Dependence of the large-scale, inner magnetospheric electric field on geomagnetic activity. J. Geophys. Res., **103**, 14959–14964.

Russell, C.T., Le, G., Chi, P., *et al*. (2000): The extreme compression of the magnetosphere on May 4, 1998, as observed by the Polar spacecraft. Adv. Space Res., **25**, 1369–1375.

Sarris, T.E, Li, X., Tsaggas, N. and Paschalidis, N. (2002): Modeling energetic particle injections in dynamic pulse fields with varying propagation speeds. J. Geophys. Res., **107** (A3), CiteID 1033, DOI 10.1029/2001JA900166.

Stern, D.P. (1975): The motion of a proton in the equatorial magnetosphere. J. Geophys. Res., **80**, 595–599.

Tsyganenko, N.A. (1989): A magnetospheric magnetic field model with a warped tail current sheet. Planet. Space Sci., **37**, 5–20.

Tu, J.-N., Tsuruda, K., Hayakawa, H. *et al*. (2000): Statistical nature of impulsive electric fields associated with fast ion flow in the near-Earth plasma sheet. J. Geophys. Res., **105**, 18901–18907.

Turner, N.E., Baker, D.N., Pulkkinen, T.I. *et al*., (2001): Energy content in the storm time ring current. J. Geophys. Res., **106**, 19149–19156.

Volland, H. (1973): A semi-empirical model of large-scale magnetospheric electric field. J. Geophys. Res., **78**, 171–180.

Wilken, B., Weiss, W., Hall, D., Grande, M., Soraas, F. and Fennell, J.F. (1992): Magnetospheric ion composition spectrometer onboard the CRRES spacecraft. J. Spacecr. Rockets, **29**, 585–591.

Zaharia, S., Cheng, C.Z. and Johnson, J.R. (2000): Particle transport and energization associated with substorms. J. Geophys. Res., **105**, 18741–18752.